

Tuning substrate-mediated magnetic interactions by external surface charging: Co and Fe impurities on Cu(111)

L. Juárez-Reyes,¹ G. M. Pastor,¹ and V. S. Stepanyuk²¹*Institut für Theoretische Physik, Universität Kassel, Heinrich Plett Straße 40, 34132 Kassel, Germany*²*Max-Planck-Institut für Mikrostrukturphysik, Weinberg 2, 06120 Halle, Germany*

(Received 11 October 2012; published 20 December 2012)

The substrate-mediated magnetic interactions between substitutional Co and Fe impurities at the Cu(111) surface have been theoretically investigated as a function of external surface charging. The modification of the interactions as a result of the metallic screening and charge rearrangements are determined self-consistently from first principles by using the Green's-function Korringa-Kohn-Rostoker method. As in the neutral Cu(111) surface, the effective magnetic exchange coupling ΔE between impurities shows Ruderman-Kittel-Kasuya-Yosida-like (RKKY) oscillations as a function of the interimpurity distance. At large interimpurity distances, the wavelength of the RKKY oscillation is not significantly affected by the value and polarity of the external surface charge. Still, important changes in the magnitude of ΔE are observed. For short distances, up to fourth nearest neighbors, surface charging offers remarkable possibilities of controlling the sign and strength of the magnetic coupling. A nonmonotonous dependence of ΔE , including changes from ferromagnetic to antiferromagnetic coupling, is observed as a function of overlayer charging. The charge-induced changes in the surface electronic structure, local magnetic moments, electronic densities of states, and interaction energies are analyzed from a local perspective. The resulting possibilities of manipulating the magnetic interactions in surface nanostructures are discussed.

DOI: [10.1103/PhysRevB.86.235436](https://doi.org/10.1103/PhysRevB.86.235436)

PACS number(s): 73.22.-f, 73.20.At, 73.20.Hb, 71.15.Mb

I. INTRODUCTION

Electrical control of magnetism at the nanoscale is currently a very active research area with a large spectrum of applications, for example, spintronics, data storage, and recording.¹⁻⁴ Important advances have been recently achieved towards the reversible tuning of magnetism controlled by means of external electric fields (EFs).^{3,5-9} For instance, Ohno *et al.* succeeded in controlling ferromagnetism in a thin-film semiconductor alloy, where ferromagnetic exchange couplings between localized magnetic moments are mediated by valence-band holes.⁵ The EF modifies the concentration of charge carriers, thus allowing us to tune the transition temperature of the hole-mediated ferromagnetic state. Moreover, applied EFs can induce switching between different magnetic states in multistable low-dimensional nanostructures.^{6,10-13} This is, for example, the case in polar magnetic molecules, where the Stark effect competes with the superexchange interaction,¹⁰ and in Fe nanochains deposited on Cu₂N/Cu(100), where magnetic switching has been triggered by a tunnel current.⁶ In supported nanoparticles, the field-induced changes in the electronic coupling between the particles and the substrate also have a strong influence on their magnetic state. Recently, a theoretical study performed by Hu *et al.* revealed that the substrate-induced spin reorientation of a Fe-phthalocyanine molecule on O-Cu(110) can be controlled by EFs.¹⁴ The importance of the substrate has been also pointed out for Ag- and Ni-supported manganese dimers¹² and in gold atoms and NO₂ molecules on graphene.¹⁵ In this context, the EF control of the deposition patterning and of ad-particle structures on graphene and MgO films has been theoretically addressed.^{15,16}

Only a few works have been so far devoted to exploring the effects of EFs on metals, where full screening is achieved within the very first surface layers. Despite the minimal

screening length, the external fields and the surface charge redistribution that it induces are likely to affect the unpaired *d*-electron states close to the Fermi energy, which are responsible for itinerant-electron magnetism in transition metals (TMs).¹⁷ Therefore, the spin-dependent screening of EFs can lead to important modifications of the magnetization and magnetic anisotropy energy (MAE) of low-dimensional ferromagnets.¹⁸ This effect has indeed been found in ultrathin ferromagnetic films, where significant changes in the MAE have been reported.^{7,19-21} Recent theoretical calculations revealed a large reduction of the magnetic moments and MAE of an Fe monolayer caused by its deposition on graphene, which can be lifted by introducing an excess of charge in the system.²² Similar manipulations have been achieved experimentally by applying a voltage across a liquid electrolyte in contact with a metallic surface.^{8,9,23} The resulting electrolytic-charge overlayer at the surface allows us to apply rather high local EFs by using relatively low voltages. For example, Weisheit *et al.* have shown that the MAE of FePt and FePd thin films can be reversibly modified by applying a voltage through an electrolyte layer.^{8,24} In a similar way, Shimamura *et al.* were able to modify the Curie temperature of ultrathin Co films by applying a gate voltage in the range of ± 2 V.⁹

Another perspective of EF control concerns the magnetic coupling mediated by metallic spacers in sandwiches and multilayers. Fechner *et al.* have theoretically shown that the relative magnetization direction of two Fe layers in a Fe/Au/Fe trilayer can be successfully switched by using an external EF, taking advantage of its contact with a ferroelectric material.²⁵ Indeed, controlling the polarization of the ferroelectric induces a spin-dependent charge screening at the interface Fe layers. The spin asymmetry modifies the phase and amplitude of the Ruderman-Kittel-Kasuya-Yosida (RKKY) interaction mediated by the Au spacer, which determines the interlayer exchange coupling. This opens novel exciting possibilities

since the RKKY interactions are present not only in metallic layered systems but also between magnetic particles deposited on metal surfaces.^{26–37} In the latter case, the magnetic interactions are often mediated by surface-state electrons, which are located precisely in the region where significant charge redistributions can be induced by external EFs. Despite the fact that these interactions are weak, of the order of a few meV, they have a strong influence on the growth of nanostructures at low temperatures.^{29,38,39} Previous theoretical investigations of the surface electronic structure of Cu(111) in the presence of EFs revealed interesting changes in the dispersion relation of the surface states, which involve modifications of the effective electron mass and Fermi wave vector.^{40–42} These results let us expect that surface charges and EFs should affect the scattering of impurities and, consequently, the interactions between them. It is therefore of considerable interest to investigate the possibility of EF manipulation of interparticle magnetic interactions by tuning the surface electron density of a noble-metal surface.

In this work, we model a charge-density accumulation on top of a Cu(111) surface by introducing an overlayer of point charges. Self-consistent *ab initio* calculations of the magnetic exchange couplings between Co and Fe substitutional surface impurities are performed for several values of overlayer charge per atom q .

The remainder of this paper is organized as follows. The next section describes the theoretical method and overlayer-charge model used in our calculations. In Sec. III the results on the magnetic exchange-interaction energy are presented and discussed. Starting from a description of the charge effects on the magnetic properties of a single substitutional impurity, we analyze the overlayer-charge dependence of the interactions between magnetic impurities in some detail. Emphasis is given to the role of the local environment of the impurities and to the redistribution of the surface electronic density induced by the electric fields. Finally, Sec. IV summarizes our conclusions and points out some relevant future studies.

II. THEORETICAL METHOD

The calculations have been performed in the framework of density-functional theory (DFT) by using the Korringa-Kohn-Rostoker (KKR) Green's-function (GF) method.⁴³ Exchange and correlation effects are treated in the local spin-density approximation (LSDA).⁴⁴ In contrast to other *ab initio* techniques, mostly based on a supercell approach, the GF-KKR method allows us to account for the surface as a truly half-infinite bulk crystal by avoiding the use of periodic boundary conditions. The effects of one or more impurities are incorporated exactly at the Kohn-Sham (KS) single-particle level by solving the Dyson equation for the perturbed GF. This allows the calculation of impurity interactions in good agreement with experiment even at large distances.²⁹ In the present study, the space is divided into atomic regions, where the atoms are represented by spherical scattering potentials enclosed by free-potential interstitial regions. Once the single-site scattering KS problem is solved inside the atomic regions, the solutions are matched within the multiple-scattering formalism. Formulated in terms of the GFs,

the self-consistent solution of the KS equations determines the electronic structure of the system. The ground-state electronic density $\rho(\mathbf{r}, \epsilon) = -1/\pi \text{Im}G(\mathbf{r}, \mathbf{r}, \epsilon)$ is then obtained from the imaginary part of the local GF $G(\mathbf{r}, \mathbf{r}, \epsilon)$.

The advantage of the GF formulation of the KKR method is the hierarchical scheme behind its construction. The surface is considered an infinite two-dimensional perturbation of the bulk crystal, and the magnetic impurities are considered a perturbation of the perfect surface. At each step the GF of the perturbed system $G(\epsilon)$ is related to the previous one $G_0(\epsilon)$ by means of the Dyson equation $G(\epsilon) = G_0 + G_0 V G$, where V is the perturbation potential describing first the vacuum and then the impurities. For the calculations reported in this work, the surface has been modeled by replacing the nuclear potentials of a six-layer-thick Cu(111) slab with vacuum spheres. The separation between the resulting two half crystals is large enough to avoid any significant electronic interactions between them. In all calculations the structure remains fixed⁴⁵ to the bulk Cu crystal having the experimental lattice constant $a = 3.615 \text{ \AA}$. Impurities and extra charges are subsequently incorporated following the same scheme, as additional perturbations to the clean surface in a real-space representation. The impurities occupy atomic sites in the topmost layer of the Cu(111) surface.⁴⁶ The overlayer charge is described by point charges q placed at the centers of the atomic spheres located at the first vacuum layer above the Cu(111) surface [see Fig. 1(a)]. Notice that these overlayer charges are treated as external potentials. Therefore, they do not participate in the self-consistent redistribution of the electronic density of the metal, which is controlled by the chemical potential of the bulk crystal. Details of the GF-KKR method can be found in previous works.^{30–32,40,43,47}

The electronic self-consistent calculations are performed for ferromagnetic (FM) and antiferromagnetic (AF) alignments between two substitutional magnetic impurities, for all values of the interparticle distance r up to 11th nearest neighbors (NNs) on the Cu(111) surface. The exchange interaction energy is then given by the difference $\Delta E =$

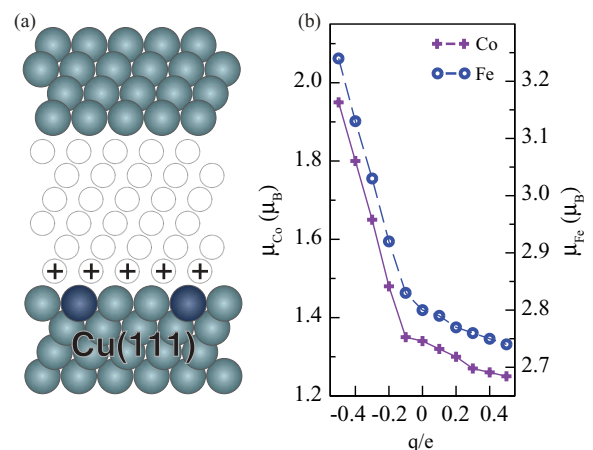


FIG. 1. (Color online) (a) Schematic diagram of the surface model. Impurities (dark spheres) and external overlayer charges (plus signs) are also depicted. (b) Calculated local magnetic moments at a single substitutional impurity as a function of overlayer charge q . The results for a Co (Fe) impurity are on the left (right) scale.

$E_{\text{FM}} - E_{\text{AF}}$ between the corresponding total energies. The overlayer charge per atom q has been varied in the range $-0.5 \leq q/e \leq 0.5$.

Let us finally recall that the focus of our study is the description of the fundamental effects of surface charging which can be used to control the interactions between surface impurities. In this study, we aim to analyze the dependence of the magnetic interactions as a function of overlayer charge accumulation. To some extent, the present model can be related to the possible effects of the charge accumulation induced by a liquid-electrolyte in contact with the surface, across which an external voltage is applied.^{8,48,49} From this perspective, the modeling of electrolyte ions as a layer of fixed-point charges q , relies on the assumption that the adsorption position and energy of the ions do not depend on the strength of the applied electrode potential.⁵⁰

III. RESULTS AND DISCUSSION

A. Single impurities

It is instructive to begin our discussion with the behavior of a single magnetic impurity. In the absence of an overlayer charge, the calculated magnetic moment of a surface substitutional Co impurity is $\mu_{\text{Co}} = 1.35\mu_B$, while for a Fe impurity it is $\mu_{\text{Fe}} = 2.80\mu_B$. These magnetic moments are largely affected by the EF generated by overlayer charges. For $q < 0$, the repulsive electrostatic potential displaces the electronic charge away from the surface into the Cu bulk, causing a reduction of the number of electrons at the Co or Fe atoms. This redistribution of charge density concerns mainly the higher-energy minority-spin states and therefore leads to the enhancement of the impurity magnetic moments. As $|q|$ increases ($q < 0$), a monotonous increase of μ_{Co} and μ_{Fe} is observed, reaching $\mu_{\text{Co}} = 1.95\mu_B$ and $\mu_{\text{Fe}} = 3.24\mu_B$ for $q = -0.5$ [see Fig. 1(b)]. For this value of q , the number of electrons at the impurity site is reduced by about 0.3 to 0.4 electrons, causing an enhancement of $0.6\mu_B$ and $0.4\mu_B$ in the magnetic moment of Co and Fe, respectively. It should be, however, noted that the decreases of electronic density and magnetic moments do not follow a linear behavior as a function of q . For instance, an overlayer charge $q = -0.1$ displaces only about 0.03 electrons at a Co impurity, enhancing μ_{Co} by less than $0.01\mu_B$ with respect to the neutral system. In contrast, by increasing $|q|$ from $q = -0.2$ to $q = -0.3$, one observes that the number of electrons inside the Co atomic sphere is reduced by nearly 0.1 and that μ_{Co} increases by about $0.17\mu_B$. A similar behavior is observed for Fe impurities.

The reason for the generally weak effect of small values of $|q|$ on the surface atoms is presumably related to the natural spill out of the surface electron density into the vacuum. In fact, in the neutral system, about 0.2 electrons per atom are found in the volume outside the atomic spheres of the surface atoms. These are basically the electrons that are displaced in order to screen the EF for small q . Consequently, the orbital occupations at the impurity are not much affected. It is only for larger values of $|q|$ that a significant electron-density depletion at the impurity occurs.

On the other hand, for positive overlayer charge $q > 0$, one observes a slight reduction of the impurity magnetic moment. The effect is, however, far less important than for $q < 0$. For instance, $\mu_{\text{Co}} = 1.25\mu_B$ and $\mu_{\text{Fe}} = 2.74\mu_B$ for the largest considered overlayer charge $q = 0.5$. In fact, the attractive potential corresponding to $q > 0$ shifts an important amount of s and p electronic density outside the surface, leading to a considerable screening of the original overlayer charge. Thus, the uppermost metal layer remains essentially neutral, and the occupation of d electronic states at the impurity site is modified to a much lower extent than for $q < 0$. As we shall see, the changes in the magnetic moments are very important for the magnetic coupling between impurities at short distances, for example, between NN impurities, where direct hybridizations are significant. At larger impurity separations, beyond second NNs, the local magnetic moments have essentially the single-impurity values. Nevertheless, the overlayer charge modifies the spin-dependent scattering potential of the surface electrons which mediate the interactions among the magnetic $3d$ atoms.

B. Impurity pair interaction

In Fig. 2 the effective exchange interaction energy $\Delta E = E_{\text{FM}} - E_{\text{AF}}$ between two Co impurities is shown as a function of the Co-Co separation distance r for different values of overlayer charge per surface atom q . Negative (positive) values of ΔE imply that a FM (AF) alignment of the impurity moments is favored. The results for Fe impurities are shown in Fig. 3. Notice that the values of r correspond to the different substitutional impurity positions at the surface. They are the same in all graphs, whereas the ranges of ΔE differ.

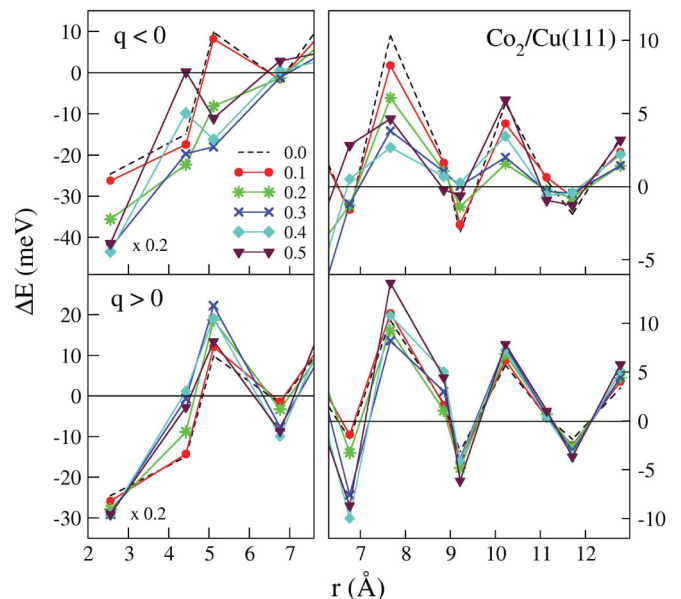


FIG. 2. (Color online) Exchange interaction energy $\Delta E = E_{\text{FM}} - E_{\text{AF}}$ between two Co impurities at the Cu(111) surface as a function of the Co-Co distance r . The upper (bottom) plot corresponds to negative (positive) surface charges per atom q . The considered absolute values of q are indicated in the inset. Note that the values of ΔE for NNs ($r = 2.55$) have been multiplied by a factor 0.2. The lines connecting the points are a guide to the eye.

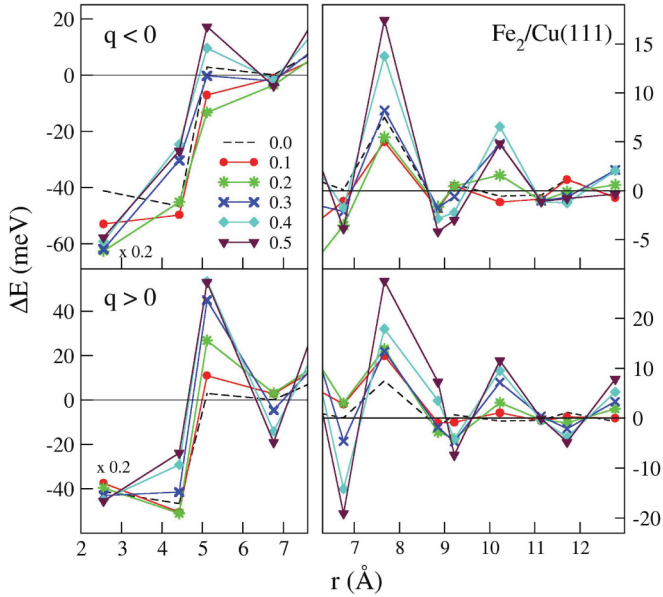


FIG. 3. (Color online) Exchange interaction energy $\Delta E = E_{\text{FM}} - E_{\text{AF}}$ between two Fe impurities at the Cu(111) surface as a function of the Fe-Fe distance r . The top (bottom) plot corresponds to negative (positive) surface charges per atom q . The considered absolute values of q are indicated in the inset. Note that the values of ΔE for NNs ($r = 2.55$) have been multiplied by a factor 0.2. The lines connecting the points are a guide to the eye.

Let us first discuss the behavior of ΔE in the absence of external charge, which corresponds to the dotted lines in Figs. 2 and 3. The results for Co and Fe impurities display the same oscillatory form, which is characteristic of an RKKY interaction. The similarity of the oscillations for both TMs indicates the common substrate-mediated interaction mechanism. Here, both surface and bulk electrons mediate the interaction between impurities.^{26,27,29} Therefore, the observed oscillation wavelength ($\approx 2.5\text{\AA}$) lies in between the values of 1.7 and 14.5 \AA expected for bulk impurities and surface adatoms, respectively.⁵¹ In the former, bulk electrons are responsible for the interactions, while in the latter only surface electrons mediate the long-range magnetic coupling. Similarly, the actual decay of the interaction amplitude differs from the $1/r^2$ and $1/r^5$ behaviors, which are typical of surface adatoms and bulk impurities.⁵¹ Notice, however, that the actual wavelength and decay ratio of the interaction can only be evaluated in the asymptotic region, at much larger interimpurity distances than those considered in this study.

In order to analyze the effects of the overlayer charge on ΔE it is meaningful to distinguish two ranges of interimpurity distance r : large separations, beyond fourth nearest neighbors ($r \gtrsim 7\text{\AA}$), where the magnetic exchange couplings are mediated by delocalized electrons, and short separations, where direct hybridizations involving localized orbitals also play an important role. Independent of the value and polarity of the overlayer charge q , the RKKY-like oscillations of ΔE are still present at large distances. While the oscillation wavelength remains essentially as in the neutral surface, the strength of ΔE is significantly modified in various ways depending on the charge polarity and on the impurity atom. For instance, positive q causes an enhancement of $|\Delta E|$ with respect to the neutral

surface, particularly in the case of Fe. However, for $q < 0$, $|\Delta E|$ is, in general, reduced for Co impurities, while it is still enhanced in the case of Fe (see Figs. 2 and 3). The changes in ΔE for large r can be of the order of 10 meV. Furthermore, one observes that surface charges $q > 0$ enhance FM as well as AF couplings for both TM impurities, while charges $q < 0$ do not significantly enhance FM interactions for any of them.

The effects of overlayer charging on the magnetic interactions become clearly stronger as the distance r is reduced. For example, if the impurities occupy any of the first four NN positions, positive q can enhance $|\Delta E|$ by more than 10 meV in the case of Co impurities and even by 40 meV in the case of Fe third-NN pairs ($r = 5.11\text{\AA}$). The largest changes in $|\Delta E|$ are generally found already for $q = 0.3$ in Co and for $q = 0.4$ in Fe. At certain distances, varying q results in a change of sign of ΔE , which allows us to tune the coupling from FM to AF and vice versa. An example of this are third-NN impurities ($r = 5.11\text{\AA}$), where $q < 0$ favors a FM alignment in both TMs (see Figs. 2 and 3). In addition, a remarkable nonmonotonous dependence of ΔE on q is observed at several distances. For instance, the third-NN Fe coupling in Fig. 3, which is weakly AF for $q = 0$, changes first to strongly ferromagnetic for small $q < 0$ ($\Delta E \simeq -12\text{ meV}$ for $q = -0.2$) and finally returns to strongly AF for $q = -0.5$ ($\Delta E \simeq 18\text{ meV}$). A similar switching of the magnetic coupling is obtained at other values of r by changing the sign of q . See, for example, the Co impurities at fourth-NN distance $r = 6.76\text{\AA}$ in Fig. 2. Therefore, a more detailed analysis of the dependence of ΔE on q is worthwhile.

In Fig. 4 the exchange interaction energy ΔE between two Co impurities (left-hand scale) and two Fe impurities (right-hand scale) is given as a function of q for the impurity positions illustrated in the insets. The dependence on q for both TMs is comparable, although $|\Delta E|$ is, in general, stronger for Fe due to its larger magnetic moment. Results for NN impurity positions are shown in Fig. 4(a). In this case, the direct electronic hybridization of the impurities is very strong and dominates their interaction. Consequently, the absolute values of ΔE are around an order of magnitude larger than for any other impurity pair. Nevertheless, the overlayer charge affects significantly the magnetic exchange since it controls the displacement of electronic density around the impurities, thus modifying the orbital occupations near the Fermi energy and the TM hybridizations. An illustrative way to analyze the behavior of ΔE for NNs impurities is to consider their interaction energy $E_{\text{int}} = E_{\text{dimer}} - 2E_{\text{single}} + E_{\text{surf}}$, where E_{single} (E_{dimer}) is the total energy of the substrate-impurity complex constituted by one (two) substitutional impurity and E_{surf} is the total energy of the unperturbed substrate. In Fig. 5 the values of E_{int} for the FM and AF states of a NN Co dimer are shown as a function of q . For $q = 0$, the attractive interaction is about one order of magnitude larger for the FM state. In the absence of external surface charge, the calculated local magnetic moment of the Co atoms in a ferromagnetic NN dimer is $\mu_{\text{Co}} = 1.45\mu_B$. For negative q , for instance, $|q| > 0.3$, this value is enhanced up to $\mu_{\text{Co}} > 1.7\mu_B$. Accordingly, $|E_{\text{int}}|$ is increased for this dimer by about 80 meV (see Fig. 5). In the AF configuration the local moments are much smaller ($\mu_{\text{Co}} = 1.24\mu_B$ for $q = 0$). Already, the smallest considered value of $q < 0$ induces an

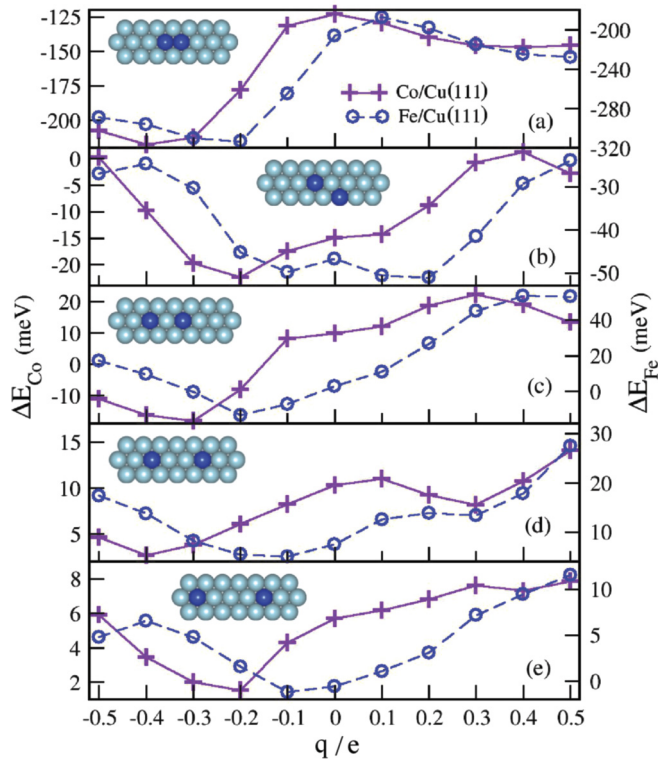


FIG. 4. (Color online) Exchange interaction energy $\Delta E = E_{\text{FM}} - E_{\text{AF}}$ of Co and Fe substitutional impurities at the Cu(111) surface as a function of the surface charge per atom q . (a)–(e) correspond to different impurity positions ordered by increasing distance, as illustrated in the insets.

enhancement of the local spin moments, which practically destabilizes this dimer configuration. In contrast, positive values of q induce a reduction of the local magnetic moments at the Co atoms. This reduction is, in fact, more pronounced in the AF configuration. However, the effect is far less important than for $q < 0$. The dimer interaction E_{int} becomes slightly more attractive for both magnetic configurations (see Fig. 5). Therefore, the results for ΔE in Fig. 4(a) are essentially dominated by the large change in E_{int} of the FM configuration for $q < 0$. In a similar way, the changes of μ_{Fe} and E_{int} for Fe NN impurities explain qualitatively the behavior observed in Fig. 4(a). The enhancement of the local spin moments for negative q can be understood as in the single impurity

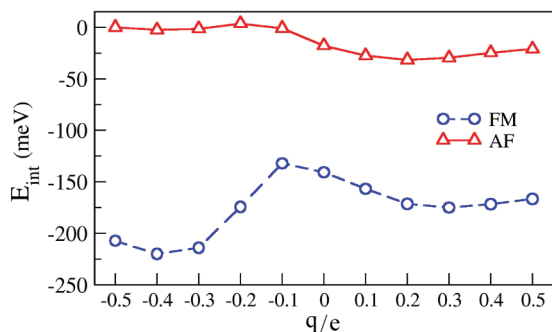


FIG. 5. (Color online) Interaction energy E_{int} between Co NN impurities as a function of overlayer charge q .

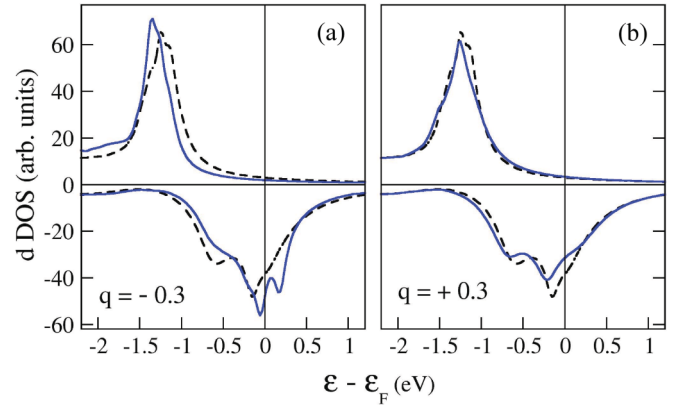


FIG. 6. (Color online) Local d -electron DOS at a Co impurity in a nearest-neighbor dimer configuration [see the inset of Fig. 4(a)]. Results are given for overlayer charges (a) $q = -0.3$ and (b) $q = 0.3$. The corresponding DOS of the neutral surface ($q = 0$) is given by the dashed curves for the sake of comparison.

case. Beyond a certain threshold (typically $|q| \geq 0.3$) the EF generated by the $q < 0$ overlayer charges causes a depletion of the electronic density at the surface layer. Thus, there are states near the Fermi energy which become unoccupied. At the impurity sites, these states are local minority-spin orbitals. Therefore, an enhancement of the impurity spin moments follows in the FM as well as in the AF configuration.

The local density of d -electron states (DOS) at a Co atom in a ferromagnetic NN dimer is shown in Fig. 6. Here, one observes that for $q < 0$ the majority-spin states are shifted towards lower energies, compared to the neutral case (dotted line). At the same time, the minority-spin band is enhanced in intensity and shifted towards higher energies. This band displays a splitting into bonding and antibonding orbitals,⁵² for which the level rearrangements occur in a different way. The bonding orbitals located at lower energies suffer a stronger shift of about 0.6 eV, while the antibonding states shift by about 0.3 eV. Nevertheless, the smaller change in the position of the antibonding subband suffices for it to cross the Fermi energy and become unoccupied. Moreover, the opposite shifts of the majority- and minority-spin bands increase the magnetic exchange splitting, thus explaining the enhancement of the local magnetic moment. For $q > 0$, the majority- and minority-spin bands show a slight displacement towards lower energies and a decrease of intensity. These changes in the DOS are related to the enhancement of $|E_{\text{int}}|$ found for $q > 0$. Notice that the FM bonding and antibonding orbitals are similarly affected. Here, the local magnetic moments are not significantly modified.

At larger interimpurity distances r (e.g., for second-NN impurity positions and beyond) the direct electronic hybridizations between the impurities are no longer relevant. The local magnetic moments at the TM atoms approach the single-impurity values as displayed in Fig. 1(b). They are essentially the same in the FM and AF configurations. At second- and third-NN positions, the key role is played by the surface Cu atoms located between the impurities. In Fig. 4(b), results are given for ΔE between second NNs as a function of the overlayer charge. For $q < 0$ one observes that the FM coupling is preserved and even slightly enhanced by small values of

$|q|$. See, for example, the results for $q = -0.1$ and -0.2 for Co pairs and $q = -0.1$ for Fe pairs. However, a remarkable nonmonotonous dependence of ΔE on q is observed for larger $|q|$. The initial decrease of ΔE is followed by a rapid increase for stronger surface charges $q < 0$, which implies a strong destabilization of the FM state. The changes in ΔE are of the order of 20 meV (30 meV) for Co (Fe) impurities. Positive overlayer charges $q > 0.2$ also tend to reduce the strength of the FM coupling. In sum, for the second-NN dimer geometry, both overlayer-charge polarities preserve the FM alignment of the impurities ($\Delta E < 0$), although the strength of the effective exchange coupling $|\Delta E|$ is drastically reduced for $|q| \geq 0.3$. In contrast, for impurities at third-NN positions [Fig. 4(c)] negative overlayer charges destabilize the AF alignment and lead to a switching of the magnetic coupling. On the other hand, for $q > 0$ the AF coupling is enhanced by about 10 meV for Co and by 40 meV for Fe.

At the second- and third-NN distances, the change in the total energy is dominated by the single-particle (SP) contribution $E_{SP} = \int^{\varepsilon_F} \eta(\varepsilon)(\varepsilon - \varepsilon_F)d\varepsilon = -\int^{\varepsilon_F} N(\varepsilon)d\varepsilon$, where $\eta(\varepsilon)$ is the electronic DOS and $N(\varepsilon) = \int^{\varepsilon} \eta(\varepsilon')d\varepsilon'$ is the integrated electronic DOS.⁵³ Consequently, the magnetic exchange energy is determined by the differences in the DOS between both magnetic configurations. However, already at second-NN distances, the local DOS at the impurity sites is not significantly affected by their relative alignment. Instead, the change in the local DOS at the Cu atoms located between the impurities plays the major role. Appreciable changes in the electronic structure are, in fact, induced at these atoms by the proximity with the TM impurities. In Fig. 7 the local density of s and p states at the Cu atom located between two third-NN Co impurities is shown [see the inset of Fig. 4(c)]. The curves are displayed for the FM and AF alignments between impurities for $q = -0.3$ and $q = 0.3$. One observes that for $q = 0.3$ the main peak in the DOS of the Cu atom between AF impurities lies at lower energies than in the case of a FM alignment [see Fig. 7(b)]. Therefore, according to the single-particle picture, an AF coupling is stabilized. This result is in agreement with the AF coupling found for $q \geq 0$. For $q = -0.3$ this peak is shifted towards higher energies [see Fig. 7(a)]. A substantial decrease of intensity is observed, reducing the SP contribution by a magnitude proportional to the locally integrated change in the density of states. As a consequence, the AF alignment

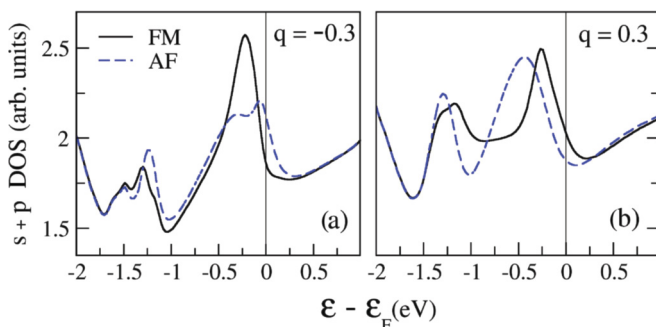


FIG. 7. (Color online) Local s - and p -electron density of states at the Cu atom located between two Co third-NN impurities. See the inset of Fig. 4(c). Results are given for overlayer charges (a) $q = -0.3$ and (b) $q = 0.3$.

is destabilized, and the magnetic coupling between impurities switches to FM ($q < 0$).

While the q dependences of ΔE for first-, second-, and third-NN distances are quite distinctive, the behaviors at larger distances show some similarities [see Figs. 4(c)–4(e)]. This suggests that the q dependence of ΔE is the result of the same microscopic mechanism, namely, a modification of the delocalized electronic density at the Cu surface. In fact, for negative values of q , the electronic density at these Cu atoms is reduced up to 0.3 electrons for $q = -0.5$, while for positive q it remains essentially unchanged. These important changes in the electronic density are responsible for the distinctive q dependence of ΔE at larger distances.

IV. CONCLUSIONS

The present study shows that the EF produced by an overlayer charge accumulation at the Cu(111) surface modifies the local magnetic properties and the interactions of surface substitutional magnetic impurities. The responses of Co and Fe impurities to external surface charging were found to be very similar. Surface charging induces a displacement of electronic density at the impurity sites, which is mainly of minority-spin character. This charge redistribution causes large modifications of the impurity local magnetic moments. Moreover, three different microscopic mechanisms have been identified to cause the changes in the magnetic exchange ΔE between atomic impurities. In the case of NN impurities, the depletion of electronic density induced by the EF at the impurity sites strongly affects the direct electronic hybridizations which determine the exchange coupling. At second- and third-NN positions on Cu(111), the electronic structures at the impurity sites are not significantly affected by the relative orientation of the impurity moments. Instead, the Cu atoms located between the impurities play the central role. The EF induces changes in the local electronic structure of these Cu atoms, which cause important variations of ΔE including the switching from FM to AF alignment of the impurities and vice versa. At larger distances, beyond fourth NNs, the strength of the substrate-mediated RKKY interaction can be modified on the order of 10 meVs. These modifications arise from the EF-induced changes in the delocalized electronic density at the Cu surface and in the scattering of the surface states at the magnetic impurities. Moreover, it has been shown that ΔE often displays a nonmonotonous dependence on the overlayer charge, which implies drastic changes in the magnetic order. In this context, a contrasting behavior of the metallic screening has been found depending on the polarity of the external surface charges.

New perspectives in the manipulation of magnetic surface nanostructures are opened by the results of the present study. For instance, the use of external surface charges and EFs to control the substitutional energies in surface alloys is certainly appealing. In fact, the modification of the binding energies of surface impurities should be helpful to control the growth of surface nanostructures and the surface growth process itself. Our results suggest that in the case of deposited magnetic particles the EF-induced reduction of the local electronic density can modify the magnetic state of the nanoparticle itself. Moreover, other magnetic properties which strongly depend on the electronic occupation at the Fermi level are expected

to suffer strong modifications as a result of external surface charging. In particular, the investigation of charging and EF effects on the magnetic anisotropy energy is of considerable interest for future applications. Finally, a further topic of future interest is the interaction of nanostructures at thin magnetic films and at highly polarizable surfaces, where external EFs are expected to strongly affect the substrate magnetic behavior.

ACKNOWLEDGMENTS

Helpful discussions with O. Brovko and P. Ruiz-Díaz are gratefully acknowledged. This work has been supported by the Deutsche Forschungs-gemeinschaft. One of the authors (L.J.R.) is supported by a Deutscher Akademischer Austausch Dienst fellowship.

-
- ¹H. Ohno, *Nat. Mater.* **9**, 952 (2010).
²E. Y. Tsymlal, *Nat. Mater.* **11**, 12 (2012).
³D. Chiba, M. Sawiki, Y. Nishitani, Y. Nakatani, F. Matsukura, and H. Ohno, *Nature (London)* **455**, 515 (2008).
⁴S. J. Gamble, M. H. Burkhardt, A. Kashuba, R. Allenspach, S. S. P. Parkin, H. C. Siegmann, and J. Stöhr, *Phys. Rev. Lett.* **102**, 217201 (2009).
⁵H. Ohno, D. Chiba, F. Matsukura, T. Omya, E. Abe, T. Dietl, T. Ohno, and K. Ohtani, *Nature (London)* **408**, 944 (2000).
⁶S. Loth, S. Baumann, C. P. Lutz, D. M. Eigler, and A. J. Heinrich, *Science* **335**, 196 (2012).
⁷T. Maruyama, Y. Shiota, T. Nozaki, K. Ohnta, N. Toda, M. Mizuguchi, A. A. Tulapurkar, T. Shinjo, M. Shiraishi, S. Mizukami, Y. Ando, and Y. Suzuki, *Nat. Nanotechnol.* **4**, 158 (2009).
⁸M. Weisheit, S. Fähler, A. Marty, Y. Souche, C. Poinsignon, and D. Givord, *Science* **315**, 349 (2007).
⁹K. Shimamura, D. Chiba, S. Ono, S. Fukami, N. Ishiwata, M. Kawaguchi, K. Kobayashi, and T. Ono, *Appl. Phys. Lett.* **100**, 122402 (2012).
¹⁰N. Baadji, M. Piacenza, T. Tugsuz, F. Della Sala, G. Maruccio, and S. Sanvito, *Nat. Mater.* **8**, 813 (2009).
¹¹C. F. Hirjibehedin, C. P. Lutz, and A. J. Heinrich, *Science* **312**, 1021 (2006).
¹²N. N. Negulyaev, V. S. Stepanyuk, W. Hergert, and J. Kirschner, *Phys. Rev. Lett.* **106**, 037202 (2011).
¹³M. C. Tropicovsky, K. Zhao, D. Xiao, Z. Zhang, and A. G. Eguiluz, *Nano Lett.* **9**, 4452 (2009).
¹⁴J. Hu and R. Wu, arXiv:1209.5453.
¹⁵Y.-H. Lu, L. Shi, C. Zhang, and Y.-P. Feng, *Phys. Rev. B* **80**, 233410 (2009).
¹⁶B. Yoon and U. Landman, *Phys. Rev. Lett.* **100**, 056102 (2008).
¹⁷L. Gerhard, T. K. Yamada, T. Balashov, A. F. Takács, R. J. H. Wesselink, M. Däne, M. Fechner, S. Ostanin, A. Ernst, I. Mertig, and W. Wulfhekel, *Nat. Nanotechnol.* **5**, 792 (2010).
¹⁸S. Zhang, *Phys. Rev. Lett.* **83**, 640 (1999).
¹⁹K. Nakamura, R. Shimabukuro, Y. Fujiwara, T. Akiyama, T. Ito, and A. J. Freeman, *Phys. Rev. Lett.* **102**, 187201 (2009).
²⁰C. G. Duan, J. P. Velev, R. F. Sabirianov, Z. Zhu, J. Chu, S. S. Jaswal, and E. Y. Tsymlal, *Phys. Rev. Lett.* **101**, 137201 (2008).
²¹M. Tsujikawa and T. Oda, *Phys. Rev. Lett.* **102**, 247203 (2009).
²²S. L. Gong, C. Duan, Z. Zhu, and J. Chu, *Appl. Phys. Lett.* **100**, 122410 (2012).
²³S. Subkow and M. Fähnle, *Phys. Rev. B* **84**, 220409(R) (2011).
²⁴H. Zhang, M. Richter, K. Koepf, I. Opahle, F. Tasnádi, and H. Eschring, *New. J. Phys.* **11**, 043007 (2009).
²⁵M. Fechner, P. Zahn, S. Ostanin, M. Bibes, and I. Mertig, *Phys. Rev. Lett.* **108**, 197206 (2012).
²⁶E. Simon, B. Újfalussy, B. Lazarovits, A. Szilva, L. Szunyogh, and G. M. Stocks, *Phys. Rev. B* **83**, 224416 (2011).
²⁷P. N. Patrone and T. L. Einstein, *Phys. Rev. B* **85**, 045429 (2012).
²⁸E. Simon, B. Újfalussy, A. Szilva, and L. Szunyogh, *J. Phys. Conf. Ser.* **200**, 032067 (2010).
²⁹V. S. Stepanyuk, A. N. Baranov, D. V. Tsviln, W. Hergert, P. Bruno, N. Knorr, M. A. Schneider, and K. Kern, *Phys. Rev. B* **68**, 205410 (2003).
³⁰O. O. Brovko, V. S. Stepanyuk, and P. Bruno, *Phys. Rev. B* **78**, 165413 (2008).
³¹O. O. Brovko, P. A. Ignatiev, V. S. Stepanyuk, and P. Bruno, *Phys. Rev. Lett.* **101**, 036809 (2008).
³²O. O. Brovko and V. S. Stepanyuk, *Phys. Status Solidi B* **247**, 1161 (2010).
³³N. Néel, R. Berndt, J. Kröger, T. O. Wehling, A. I. Lichtenstein, and M. I. Katsnelson, *Phys. Rev. Lett.* **107**, 106804 (2011).
³⁴L. Zohu, J. Wiebe, S. Lounis, E. Vedmedenko, F. Meier, S. Blügel, P. H. Dederichs, and R. Wiesendanger, *Nature Physics* **6**, 187 (2010).
³⁵F. Meier, L. Zhou, J. Wiebe, and R. Wiesendanger, *Science* **320**, 82 (2008).
³⁶P. Wahl, P. Simon, L. Diekhöner, V. S. Stepanyuk, P. Bruno, M. A. Schneider, and K. Kern, *Phys. Rev. Lett.* **98**, 056601 (2007).
³⁷A. A. Khajetoorians, J. Wiebe, B. Chilian, and R. Wiesendanger, *Science* **332**, 1062 (2011).
³⁸V. S. Stepanyuk, L. Niebergall, R. C. Longo, W. Hergert, and P. Bruno, *Phys. Rev. B* **70**, 075414 (2004).
³⁹X. P. Zhang, B. F. Miao, L. Sun, C. L. Gao, A. Hu, H. F. Ding, and J. Kirschner, *Phys. Rev. B* **81**, 125438 (2010).
⁴⁰P. A. Ignatiev and V. S. Stepanyuk, *Phys. Rev. B* **84**, 075421 (2011).
⁴¹K. Berland, T. L. Einstein, and P. Hyldgaard, *Phys. Rev. B* **85**, 035427 (2012).
⁴²P. A. Ignatiev, O. O. Brovko, and V. S. Stepanyuk, *Phys. Rev. B* **86**, 045409 (2012).
⁴³K. Wildberger, V. S. Stepanyuk, P. Lang, R. Zeller, and P. H. Dederichs, *Phys. Rev. Lett.* **75**, 509 (1995).
⁴⁴S. Vosko, L. Wilk, and N. Nusair, *Can. J. Phys.* **58**, 1200 (1980).
⁴⁵Structural relaxations have been explored in a five-layer Cu(111) slab, using the Vienna Ab initio Simulation Package (VASP).⁵⁴ Calculations were performed for a neutral system and for a total charge imbalance of ± 0.3 electrons per surface atom. The resulting relaxations were found to be similar in the three considered cases. These structural changes are not expected to affect the main results of this paper.
⁴⁶P. Wahl, A. P. Seitsonen, L. Diekhöner, M. A. Schneider, and K. Kern, *New. J. Phys.* **11**, 113015 (2009).

- ⁴⁷J. Zabloudil, R. Hammerling, L. Szunyogh, and P. Weinberger, *Electron Scattering in Solid Matter: A Theoretical and Computational Treatise*, Springer Series in Solid-State Sciences Vol. 147 (Springer, Berlin, 2005).
- ⁴⁸Y. Yamada, K. Ueno, T. Fukumura, H. T. Yuan, H. Shimotani, Y. Iwasa, L. Gu, S. Tsukimoto, Y. Ikuhara, and M. Kawasaki, *Science* **332**, 1065 (2011).
- ⁴⁹I. Žutić and J. Černe, *Science* **332**, 1040 (2011).
- ⁵⁰S. Schnur and A. Groß, *Catal. Today* **165**, 129 (2011).
- ⁵¹P. Hylgaard and M. Persson, *J. Phys. Condens. Matter* **12**, L13 (2000).
- ⁵²S. Alexander and P. W. Anderson, *Phys. Rev.* **133**, A1594 (1964).
- ⁵³B. Drittler, M. Weinert, R. Zeller, and P. H. Dederichs, *Phys. Rev. B* **39**, 930 (1989).
- ⁵⁴G. Kresse and J. Hafner, *Phys. Rev. B* **47**, 558 (1993); **49**, 14251 (1994).